ARCHIVE OF MECHANICAL ENGINEERING

DOI: 10.24425/ame.2026.1880 2026, Vol. 73, No. 3, pp. 429–448

Hojjat ASHOURI [1]

The impact of viscous behavior on thermo-mechanical fatigue life of cylinder head using two-layer viscoplasticity model

Received 25 February 2025, **Revised** 31 May 2026, **Accepted** 7 June 2026, **Published online** 6 July 2026

Keywords: viscous behavior effect, two-layer viscoplasticity model, TMF life, cylinder head

The cylinder head is a fundamental and challenging part of an engine, in which the thermo-mechanical stresses due to fatigue effectively contribute to its damage and reduction of its fatigue life. This study investigated the effect of viscous behavior on the thermomechanical fatigue life of a cylinder head using the Sehitoglu model, with the finite element method employed for the analysis. The ABAQUS software was also used to predict temperatures, stresses, and thermomechanical fatigue life using the Sehitoglu model and the FEMFAT software. Moreover, a two-layer viscoplasticity model was employed to account for the cylinder head's viscous behavior. Low-cycle fatigue tests were carried out at various temperatures to characterize the viscous and mechanical behavior of the aluminum-silicon-magnesium alloy. The finite element analysis suggested that the maximum temperature of 308°C and the maximum stress of 136 MPa occurred at the valve bridge. The fatigue life analysis revealed that neglecting viscous behavior led to a 657-cycle (8.9%) overestimation of fatigue life, emphasizing the importance of incorporating viscous behavior into the thermo-mechanical fatigue life analysis.

1. Introduction

Nowadays, internal combustion engines are among the substantial components of the advanced industries. Currently, the main goal of automotive companies is to design and manufacture more powerful engines with lower fuel consumption, emissions, and weight [1, 2]. As a crucial engine part, the cylinder head is exposed to combustion gases, lubricating, and cooling fluids [3, 4]. With its complex geometry, this component is subjected to oscillating thermal and mechanical loads,

✉ Hojjat ASHOURI, e-mail: ha.ashouri@iau.ac.ir

[1]Department of Mechanic, VaP.C., Islamic Azad University, Varamin, Iran

© 2026. The Author(s). This is an open-access article distributed under the terms of the Creative Commons Attribution (CC-BY 4.0, https://creativecommons.org/licenses/by/4.0/), which permits use, distribution, and reproduction in any medium, provided that the author and source are cited.

highlighting the significance of its material. The cylinder head material must possess sufficient thermal and mechanical strength to tolerate the thermomechanical stresses of combustion pressure and gas heat, underscoring the necessity of its thermomechanical analysis and fatigue life prediction [5, 6].

The literature reports several studies related to cylinder head stress analysis and fatigue life. A study by Ashouri et al. on cylinder head cracks using the two-layer viscoplasticity model showed that the bridge between intake and exhaust valves of the cylinder head are subjected to low-cycle fatigue [7]. In another study on the impact of thermal barrier coating on the thermo-mechanical stresses of the cylinder head using the same model, Ashouri proved that the thermal barrier coating can reduce the temperature and stress distribution on the cylinder head, improving its fatigue life [8]. Young et al. predicted the thermo-mechanical fatigue life of the cylinder head using the Sehitoglu model, revealing the significant role of mechanical damage in the thermomechanical fatigue life [9]. Using the cumulative damage model, Liu et al. predicted the thermomechanical fatigue life of the cylinder head. Their results suggested that the creep damage can be neglected in the thermomechanical fatigue life analysis [6].

Basiri and Amini applied various criteria to analyze the cylinder head low-cycle fatigue (LCF) life, and reported the Ostergren modified model as the most accurate one in predicting the cylinder head fatigue life [10]. Another study on the thermomechanical fatigue life of a diesel engine's cylinder head, conducted by Lu et al., showed less than 10% diffrence between the experimental and simulation results [3]. A model presented by Hazime et al. to evaluate the thermo-mechanical fatigue life of an iron cylinder head suggested a very good fit between the experimental results and fatigue life predicted using this method [11]. The prediction of thermomechanical fatigue life of an aluminum cylinder head by Hazimeh et al. showed a higher fit between the predicted fatigue life and experimental results by considering the porosity [5]. The reliability of the fatigue life based on the neural network was evaluated by Jing et al., suggesting that the fatigue life of a cylinder with 95% reliability would be approximately 75 hours [12].

In a study on the impact of porosity defects on the cylinder head crack initiation in a diesel engine, Li et al. reported inlet and outlet ducts, along with water channels of the cylinder head, as critical areas [1]. Ashouri assessed the quenching process on the LCF life of the cylinder head. The finite element method (FEM) results demonstrated the nonnegligible and significant impact of residual stresses due to the quenching process on the LCF life [13]. By applying the 400-h durability test, Ashouri reported no rupture possibility throughout the cylinder head [14]. The prediction of Zhang et al. on LCF life revealed the significant impact of thermal loading on the initiation of LCF in the cylinder head [15]. The simulation conducted by Mahajan et al. to analyze the cylinder head high-cycle fatigue (HCF) life suggested that the bridge between the valves is prone to fatigue cracks [16]. In another prediction on the cylinder head thermo-mechanical fatigue life, Seifert et

al. reported a very good fit between the critical areas in the fatigue analysis and the crack points in the experimental test [17].

The simulation performed by Zeng et al. to predict the thermomechanical fatigue life using the Sehitoglu model revealed the considerable role that oxidation damage plays on the thermo-mechanical fatigue life of the cylinder head [18]. Pingale et al. evaluated the HCF life of the cylinder head using modified Goodman criteria, in which the high-cycle safety factor distribution showed no critical area in the cylinder head [19]. Ren et al. evaluated the HCF life of the aluminum cylinder head using fatigue tests and microscopic observations and reported water channels as a critical area [4]. Moreover, Blondet and Barthoux developed a software to evaluate the truck's cylinder head fatigue life and provide a more accurate prediction of fatigue life [20]. Mahjan et al. optimized the bridge between the cylinder head's valves to enhance its fatigue life. The optimization proposed the water channels as critical areas and reduced HCF damage in such areas by approximately 6.5% [21].

Bronger et al. proposed a pattern to include the impact of cylinder head thermal aging on fatigue life. According to their findings, excluding the aging impact leads to overestimation of cylinder head fatigue life [22]. Ashouri studied the mechanical, oxidation, and creep damages on the thermomechanical fatigue life using the Sehitoglu model, suggesting the substantial effect of mechanical damage on the cylinder head fatigue life [23]. Ashouri also studied the impact of viscosity stress on the LCF life using the Morrow model. The findings revealed that excluding the effect of viscosity stress leads to an overestimation of LCF (approximately 5.9%) [24]. The cylinder head optimization using the sub-modeling technique was performed by Houang et al., showing the water channels as critical areas [25]. Pierjiacomi et al. predicted the cylinder head fatigue life regarding the boiling effect, in which the safety factor distribution showed no critical area in the cylinder head [26].

Due to limited data on material hardening, softening, and viscous behavior, the stress and fatigue analyses performed on the cylinder head are mainly based on simple behavioral models, such as elastic-plastic, with less focus on the impact of viscous behavior. Significantly, aluminum alloy exhibits viscous behavior at engine operating temperatures [7, 27, 28]. Thus, this study used the two-layer viscoplasticity model to simulate and evaluate the thermo-mechanical behavior and the viscous behavior of the cylinder head, respectively, and analyze its thermo-mechanical fatigue life by employing the Sehitoglu model. First, the ABAQUS software was employed to model and mesh the cylinder head. The parameters of the two-layer viscoplasticity model were extracted using the LCF test at various temperatures. Then, ABAQUS software was applied to analyze the thermo-mechanical stresses. Eventually, the impact of viscous behavior on the thermomechanical fatigue life of the cylinder head was evaluated using the Sehitoglu model and FEMFAT software.

2. Methodology

2.1. The material and its behavioral model

The present study investigated and simulated the thermo-mechanical behavior of aluminum-silicon-magnesium cast alloy to be applied in the cylinder head. Selecting an appropriate model to evaluate the thermomechanical fatigue of materials is predominantly significant. The two-layer viscoplasticity pattern was employed to simulate aluminum alloy behavior and analyze its plastic and viscous behavior (Fig. 1).

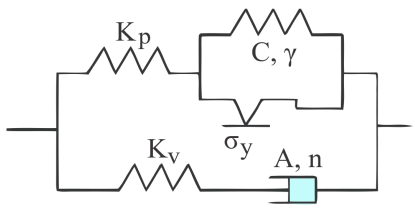

Fig. 1. The two-layer viscoplasticity model [29]

This model divides the plastic and viscous effects into two elastic-plastic and elastic-viscous networks [29]. The two-layer viscoplasticity model is the most appropriate model to analyze the response of materials, such as an aluminum cylinder head, which exhibits considerable temperature- and plastic-dependent behavior at high temperatures [27, 28]. As a proper model for plastic behavior in materials, the hardening nonlinear isotropic-kinematic pattern of Chaboche was employed in the plastic network, which can predict behaviors such as hardening, softening, creep, and mean stress relaxation [28, 29]. The Nonlinear isotropic/kinematic hardening Chaboche model includes motion of the yield surface proportional to the value of X in the stress zone, and also changes in the size of the yield surface are proportional to the plastic strains, as shown in the following equation [30]:

$$\dot{X} = C\frac{1}{\sigma_0}\left(\sigma_{ij} - X_{ij}\right)\dot{\bar{\varepsilon}}^{\mathrm{PL}} - \gamma_{ij}\dot{\bar{\varepsilon}}^{\mathrm{PL}} + \frac{1}{C}\dot{C}X_{ij}\,, \tag{1}$$

where σ^0, $\dot{\bar{\varepsilon}}^{\mathrm{PL}}$, C, γ, and $\dot{C}$ represent the size of the yield surface, the rate of equivalent plastic strain, material constants, and the exchange rate of C with temperature, respectively. The following equation was used to define the isotropic part, in which b and Q are material constants [30]:

$$R = Q\left(1 - \exp\left(-b\dot{\bar{\varepsilon}}^{\mathrm{PL}}\right)\right). \tag{2}$$

The yield criterion for this model was achieved using [30]:

$$f = |\sigma - X| - k - R, \tag{3}$$

where σ, k, and R represent the stress, the initial yield stress value, and the isotropic hardening variable, respectively. The Norton-Hoff law was used to consider the effect of strain rate, as follows [27]:

$$\dot{\varepsilon}_V = A(\sigma_V)^n, \tag{4}$$

where the $\dot{\varepsilon}_V$ and σ_V represent viscous strain rate and viscous stress, respectively, and A and n are material constants. The rate of the elastic moduli in the two viscous and plastic networks is expressed by f. Where k_v and k_p represent elastic moduli in the elastic-viscous and elastic-plastic networks, respectively [29]:

$$f = \frac{k_v}{k_v + k_p}. \tag{5}$$

2.2. The finite element model and material properties

Traditionally, the engine parts optimization was based on prototypes and various tests. Such an approach is costly, time-consuming, and challenging because it requires the production and testing of multiple prototypes at the initial stages of design. Notably, such problems have been solved through using the finite element analysis (FEA) to evaluate the efficacy of different designs [7, 15]. As shown in Fig. 2, the cylinder heads analyzed in the present study were made of aluminum alloy. The two valve guides are made of steel alloy, with a Young's modulus of 106 GPa and a Poisson's ratio of 0.35. The three valve seats are made of steel, with a Young's modulus of 200 GPa and a Poisson's ratio of 0.3 [31, 32]. The model consists of 65580 nodes and approximately 80000 degrees of freedom.

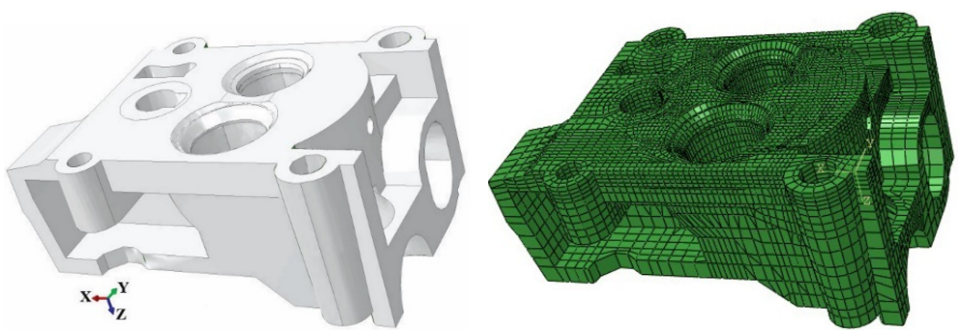

(a) (b)

Fig. 2. (a) cylinder head and (b) finite element model of the cylinder head [31]

2.3. Thermo-mechanical boundary conditions

Thermo-mechanical analysis was performed in two steps, including thermal and mechanical analyses to calculate temperature distribution and thermomechanical stress, respectively. At the first step, the region between the intake and exhaust

valves with the highest temperature concentration was subjected to thermal loadings with minimum and maximum temperatures of 35°C and 300°C. The thermal analysis was performed to determine the temperature distribution by defining the thermal transfer properties, specific heat, and conductivity factors. This analysis consists of three cycles to achieve a stable thermal response, and each cycle contains two parts: heating the cylinder head to its maximum operational temperature and cooling it to its minimum operational temperature by *CFLUX and *FILM subroutines. In other words, the boundary conditions were inserted into the ABAQUS software as a file with a *.inp extension. In the mechanical analysis, it is assumed that the cylinder head is securely fixed to the engine block through the four bolt holes, so the nodes along the base of the four bolt holes are secured in all directions during the entire simulation [31, 32]. The boundary conditions for the cylinder head in the mechanical analysis are shown in Fig. 3.

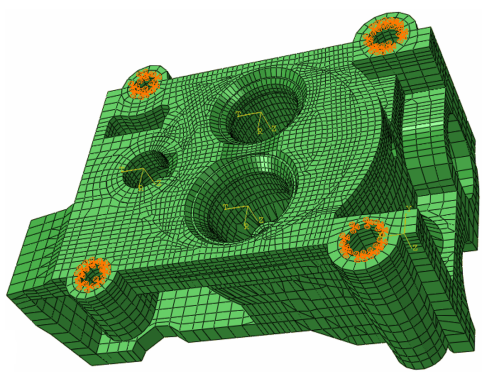

Fig. 3. Boundary conditions in mechanical analysis

2.4. Model for thermo-mechanical fatigue life prediction

Based on the Sehitoglu theory, the total damage, (D^{total}) of components withstand thermo-mechanical stress would be the sum of mechanical (D^{mech}), oxidation (D^{ox}), and creep (D^{creep}) damages [33, 34]:

$$D^{\text{total}} = D^{\text{mech}} + D^{\text{ox}} + D^{\text{creep}}. \tag{6}$$

Based on the Basquin-Coffin-Manson relationship, the mechanical strain range $\Delta\varepsilon$ of cyclic deformation would be [35]:

$$\Delta\varepsilon = \frac{\sigma'_f}{E}(2N_f)^b + \varepsilon'_f(2N_f)^c, \tag{7}$$

where $\Delta\varepsilon$, σ'_f, E, $2N_f$, b, ε'_f, and c represent the strain amplitude, the fatigue strength coefficient, the elasticity modulus, the number of reversals to failure,

the fatigue strength exponent, the fatigue strength coefficient, the fatigue ductility exponent, respectively. The oxidation damage was calculated using the following equation [34]:

$$D^{\mathrm{ox}} = \left[\frac{h_{\mathrm{cr}}\delta_0}{B\phi^{\mathrm{ox}}K_p^{\mathrm{eff}}}\right]^{\frac{-1}{\beta}} \frac{2\left(\Delta\varepsilon_{\mathrm{mech}}\right)^{\left(\frac{2}{\beta}\right)+1}}{\dot{\varepsilon}_{\mathrm{mech}}^{1-(\alpha/\beta)}}, \tag{8}$$

where h_{cr}, δ_0, α and B represent the material parameters, while $\dot{\varepsilon}_{\mathrm{mech}}$ and K_p^{eff} represent mechanical strain rate, respectively [34]:

$$K_p^{\mathrm{eff}} = \frac{1}{t_c}\int_0^{t_c} D_0 \exp\left(\frac{-Q}{RT(t)}\right) \mathrm{d}t. \tag{9}$$

where D_0, Q, and R represent material parameter, oxidation activation energy, and the universal gas constant, respectively. The oxidation phasing factor can be expressed using the following equation [34]:

$$\Phi^{\mathrm{ox}} = \frac{1}{t_c}\int_0^{t_c} D_0 \exp\left[\frac{-1}{2}\left(\frac{\left(\frac{\dot{\varepsilon}_{\mathrm{th}}}{\dot{\varepsilon}_{\mathrm{mech}}}\right)}{\xi^{\mathrm{ox}}}\right)^2\right] \mathrm{d}t, \tag{10}$$

where ξ^{ox} and $\dot{\varepsilon}_{\mathrm{th}}$ represent the proportion of damage associated with differing phases and the rate of thermal strain, respectively. Creep damage, resulting from mechanisms such as void growth and grain boundary cracking, is described by the following equation [34]:

$$D^{\mathrm{creep}} = \Phi^{\mathrm{creep}} \int Ae^{\left(-\frac{\Delta H}{RT}\right)} \left(\frac{\alpha_1\overline{\sigma} + \alpha_2\sigma_H}{K}\right)^m \mathrm{d}t, \tag{11}$$

where Ae, m, ΔH, $\overline{\sigma}$, σ_H, and K denote material constants, creep activation energy, equivalent stress according to Mises, hydrostatic stress, and drag stress, respectively. Also, α_1 and α_2 representing scaling factors of the relative proportion of damage due to the tensile and compressive stress. Moreover, Φ^{creep} is the creep phase factor [34]:

$$\Phi^{\mathrm{creep}} = \frac{1}{t_c}\int_0^{t_c} \exp\left[\frac{-1}{2}\left(\frac{\left(\frac{\dot{\varepsilon}_{\mathrm{th}}}{\dot{\varepsilon}_{\mathrm{mech}}}\right) - 1}{\xi^{\mathrm{creep}}}\right)^2\right] \mathrm{d}t. \tag{12}$$

where ξ^{creep} represents the sensitivity of the phase shift to creep damage. The thermo-mechanical fatigue (TMF) life prediction procedure encompasses thermal, mechanical, and fatigue damage analyses, as shown in Fig. 4.

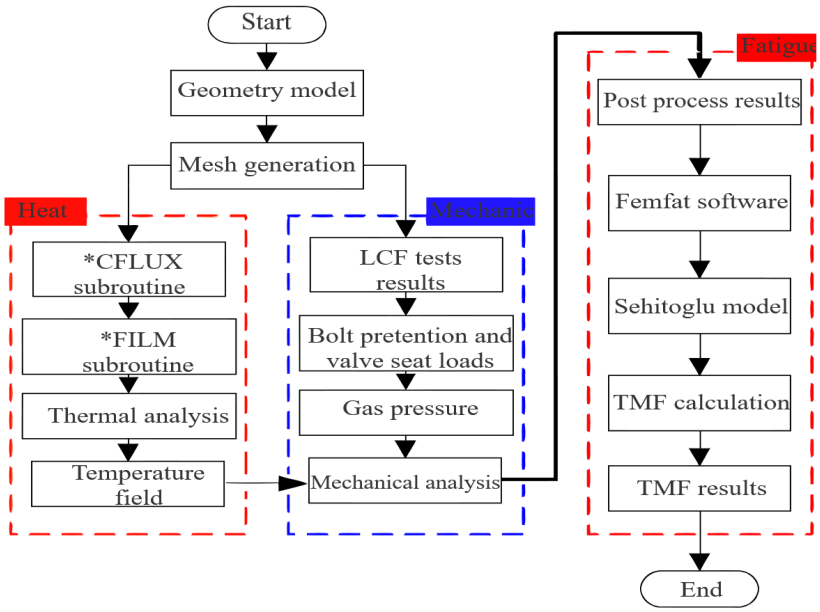

Fig. 4. Flowchart of the TMF analysis procedure

2.5. Experimental and simulation LCF tests

The aluminum alloy consisted of 8.3 wt.% Si, 0.33 wt.% Mg, 0.98 wt.% Fe, 3.13 wt.% Cu, 0.66 wt.% Zn, 0.64 wt.% Mn, 0.03 wt.% Ti, with the balance being Al. The LCF testing setup is displayed in Fig. 5. As illustrated, an induction system was employed to heat the specimens. Mechanical strain at elevated

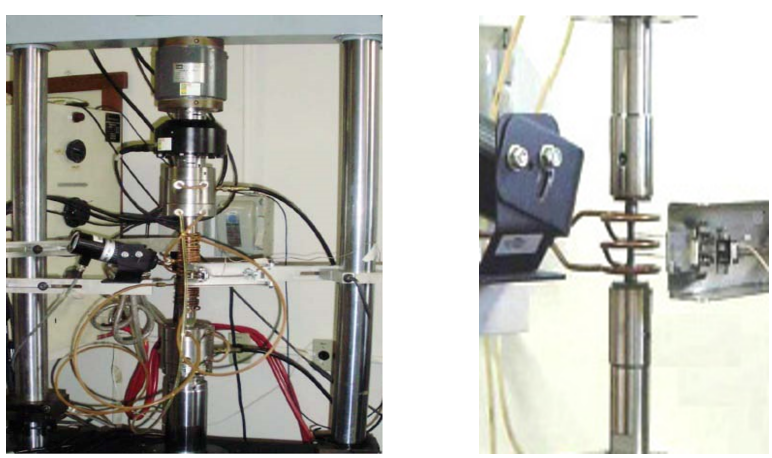

(a) (b)

Fig. 5. (a) Material testing machine MTS 810 and (b) induction heater and extensometer

temperatures was measured using an extensometer and controlled via computer. The strain rate was maintained at $1 \cdot 10^{-3}$ 1/s for all temperatures. To simulate the LCF tests, the intended sample in the low-cycle fatigue experimental test is modeled using SolidWorks software, the dimensions of which are shown in Fig. 6, and then imported into ANSYS software. After meshing, the mechanical strain is applied, similar to the low-cycle fatigue experimental test conditions. Eventually, the simulated stress-strain curve is drawn.

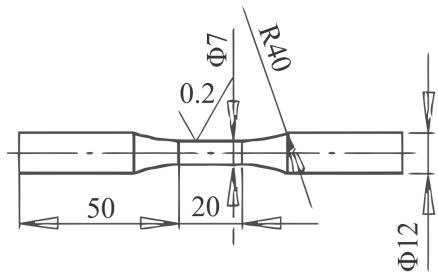

Fig. 6. The geometry of LCF test specimens and their details (dimensions in mm)

3. Results and discussion

3.1. LCF tests results

LCF test results of the aluminum cylinder heads at 100 and 300°C, which were also simulated using Ansys software, are shown in Fig. 7, indicating a very good fit between the experimental and simulated fatigue results. Tables 1 and 2 contain the kinematic and isotropic hardening parameters of the cylinder head material based

Table 1. Kinematic hardening parameters

C_1@100°C (MPa)	79993
C_1@300°C (MPa)	76850
C_2@100°C (MPa)	64327
C_2@300°C (MPa)	11810
C_3@100°C (MPa)	11743
C_3@300°C (MPa)	7858
γ_1@100°C (–)	1063
γ_1@300°C (–)	353
γ_2@100°C (–)	4206
γ_2@300°C (–)	590
γ_3@100°C (–)	862
γ_3@300°C (–)	655

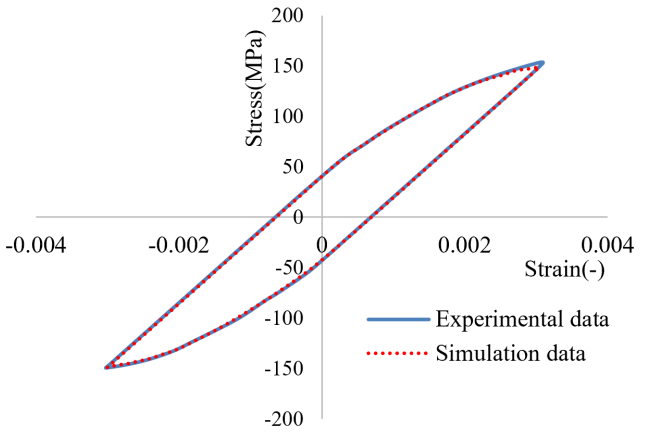

(a)

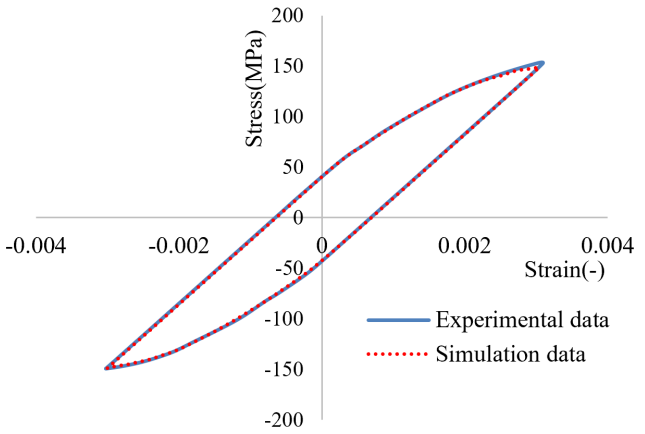

(b)

Fig. 7. The cylinder head material's cyclic behaviors at (a) 100°C and (b) 300°C

Table 2. Isotropic hardening parameters and elastic modulus

E@100°C (GPa)	64.7
E@300°C (GPa)	51.7
k@100°C (MPa)	101.9
k@300°C (MPa)	48.1
Q@100°C (MPa)	21.25
Q@300°C (MPa)	-32.62
b@100°C (–)	8.6
b@300°C (–)	1.9

on LCF tests. Moreover, Table 3 presents the viscous parameters in the two-layer viscoplasticity model.

Table 3. Viscous behavior parameters

A@100°C ($MPa^{-n}sec^{-1}$)	$1.53 \cdot 10^{-5}$
A@300°C ($MPa^{-n}sec^{-1}$)	$6.32 \cdot 10^{-8}$
n@100°C (–)	1.63
n@300°C (–)	1.63
f@100°C (–)	0.18
f@300°C (–)	0.016

3.2. Thermal analysis

Thermal analysis aims to find the cylinder head's temperature field. The principal stresses are due to thermal loading. The remaining stresses would result from the combustion pressure and mechanical restraints. Therefore, thermal analysis would be the principal analysis in terms of predicting the fatigue life of the cylinder head. Fig. 8 presents the temperature distribution at the end of the engine heating cycle.

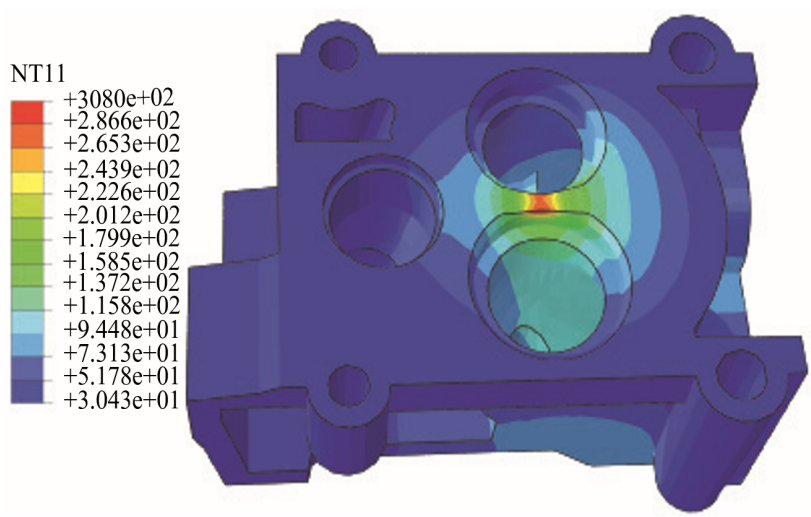

Fig. 8. The temperature distribution in the cylinder head

The highest temperature was recorded at 308°C at the bridge between the intake and exhaust valves. This peak arises from the convergence of combustion gases in this region, aligning with [12, 18, 32]. The thermal results can be used to identify critical areas. Therefore, the results suggested the critical nature of the

intake and exhaust valves bridge. Temperature variation in the critical region over time is shown in Fig. 9, indicating a single on/off cycle of the engine.

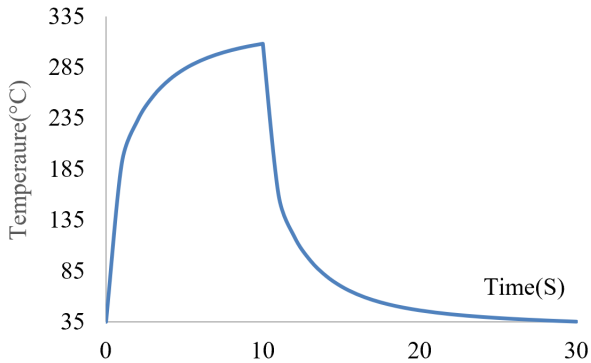

Fig. 9. The temperature in the critical area

3.3. Mechanical analysis

Mechanical analysis was performed in two steps, commencing by compressing three valve seats in the cylinder head channels. A static analysis procedure is used for this purpose. The temperatures of various nodes of the cylinder head in the thermal analysis of a single thermal cycle are stored for mechanical analysis, which consists of the cylinder head heating to its maximum temperature and then its reduction to the ambient temperature. In other words, in the mechanical analysis, the temperature of different cylinder head nodes calculated in thermal analysis, along with other forces that the cylinder head tolerates during its operational cycle, are considered for different nodes. The second step contains the application of the achieved temperature distribution along with combustion and bolt pre-load. Fig. 10 illustrates Von-Mises stress distribution in the cylinder head, showing the maximum Von-Mises stress of 136 MPa at the region between the intake and exhaust valves.

The equivalent plastic strain distribution is presented in Fig. 11, which indicates the entrance of cylinder head material into the yield region by providing a value greater than zero. The equivalent plastic strain is an index to determine the critical points. Examining Fig. 11 shows the region between that the intake and exhaust valves is critical and prone to fatigue cracks.

The Von-Mises stress distribution in the cylinder head without considering viscous behavior is shown in Fig. 12, where the maximum Von-Mises stress of 130.2 MPa occurred at the bridge between the intake and exhaust valves. Examining Figs. 10 and 12 reveals that the maximum Von-Mises stress with and without considering viscous behavior was 136 and 130.2 MPa, respectively. In other words, excluding viscous behavior leads to an underestimation of Von-Mises stress by 5.8 MPa (or 4.3%).

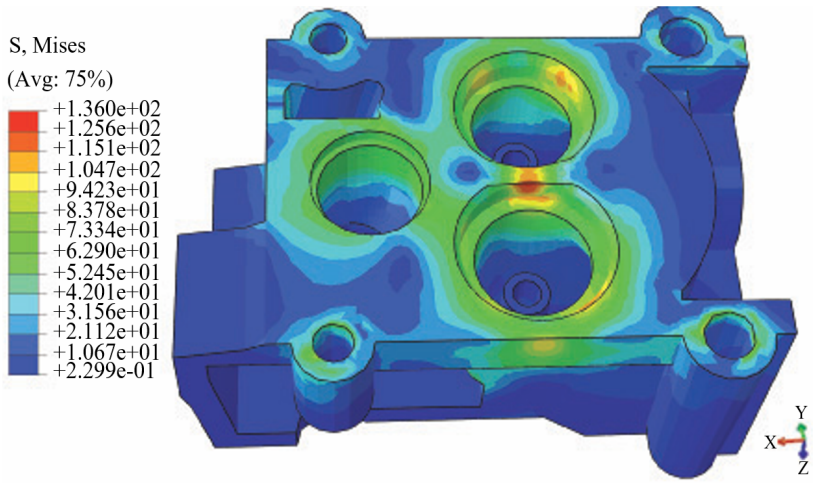

Fig. 10. The Von-Mises stress distribution in the cylinder head considering viscous behavior

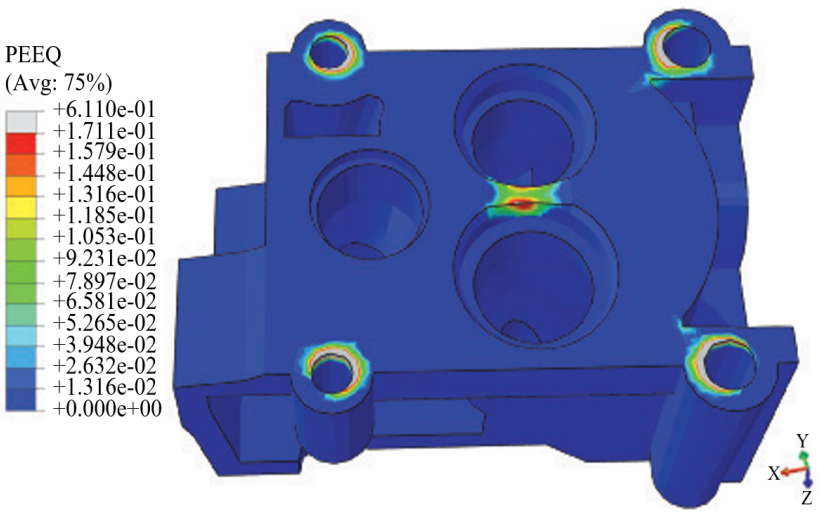

Fig. 11. The plastic strain distribution

In Fig. 13, the normal stress diagram (σ_{xx}) at the bridge between intake and exhaust valves for the critical node is shown with and without considering the viscous behavior. According to this figure, the maximum temperature occurred at the tenth second of the operation (Fig. 9), which was a compressive stress due to the thermal loading and combustion pressure. On the other hand, the stress turned into tensile type by engine shutdown and gradual temperature reduction due to the assembly loads.

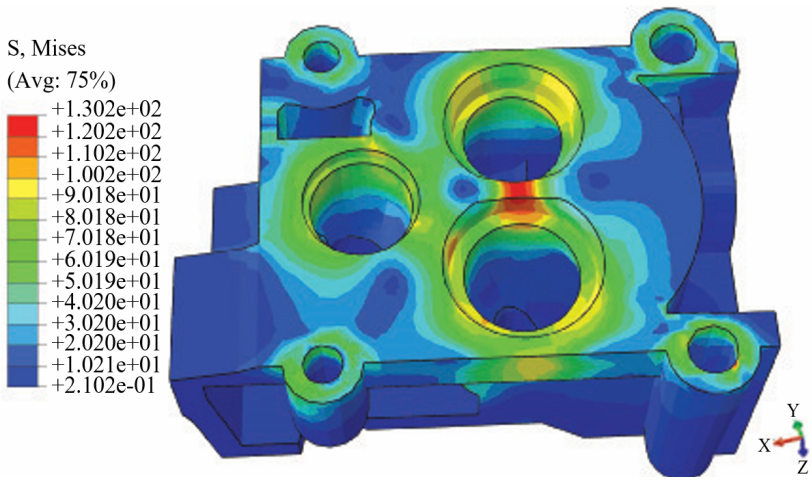

Fig. 12. The Von-Mises stress distribution without considering viscous behavior

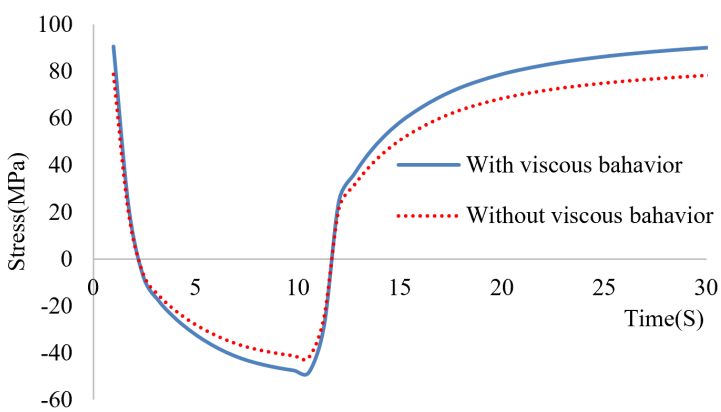

Fig. 13. The normal stress in the X direction for critical point versus time

3.4. Thermo-mechanical fatigue life prediction

Many of the engineering components encounter failure in their operational conditions under oscillating loading and high temperatures, showing the vital importance of the appropriate prediction of the lifetime of components. Therefore, the life prediction models, such as the Sehitoglu model, should be employed to calculate the TMF life of a material [8, 18, 23]. The Sehitoglu model constants and thermo-mechanical analysis results were entered into the FEMFAT software to evaluate the TMF life. The thermo-mechanical fatigue analysis results of the cylinder head using the Sehitoglu model are shown in Fig. 14. The lowest TMF life was 7407 cycles (1/0.000135 = 7407), which occurred in the region between the intake and exhaust valves, making it a critical area. Moreover, the critical ar-

eas in thermomechanical and fatigue life analyses are aligned. Fig. 15 displays the thermo-mechanical fatigue life analysis results of the cylinder head without considering viscous behavior, where the lowest fatigue life was 8064 cycles at the bridge between the intake and exhaust valves. Figs. 14 and 15 indicate that

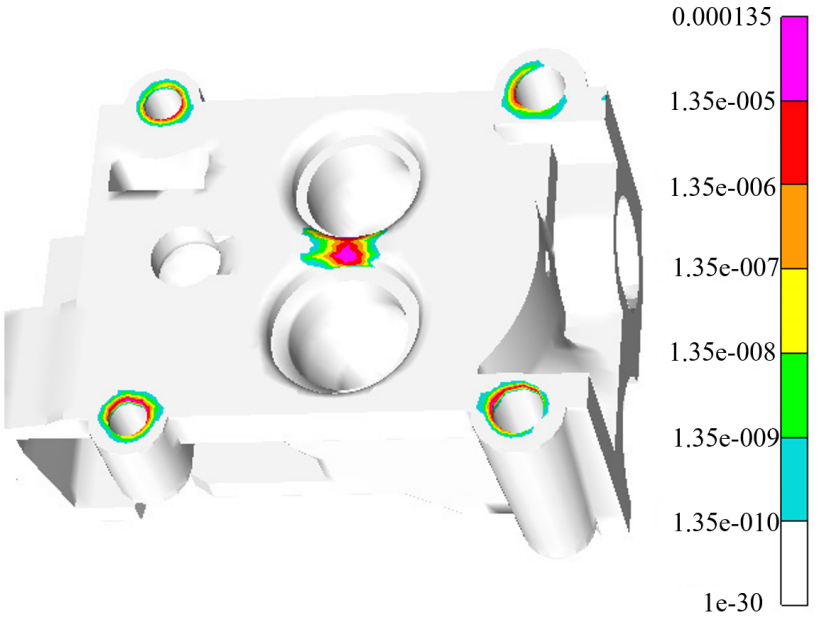

Fig. 14. The TMF life prediction in the cylinder head considering viscous behavior

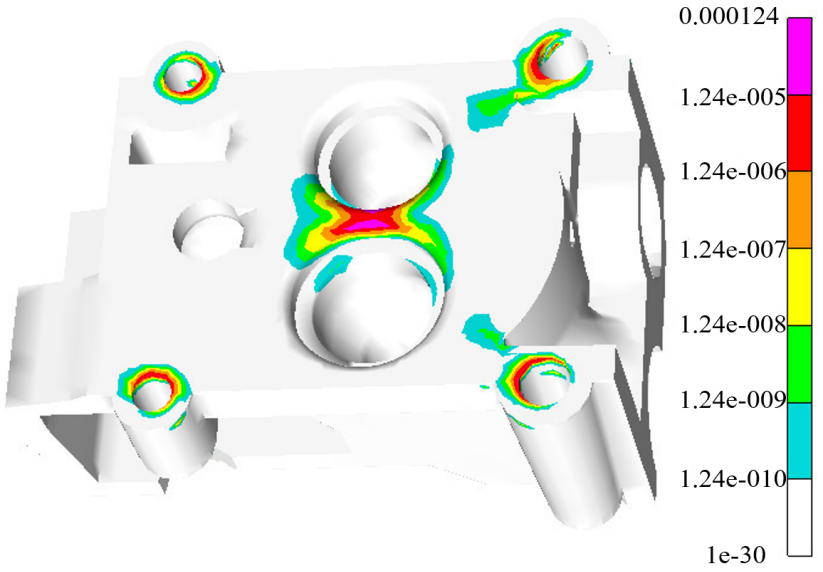

Fig. 15. The TMF life prediction in the cylinder head without considering viscous behavior

the minimum TMF life with and without considering the viscous behavior was 7407 and 8064 cycles, respectively. In other words, excluding the viscous behavior leads to 657 cycles (or 8.9%) overestimation of cylinder head thermomechanical fatigue life, highlighting the necessity of considering the viscous behavior in the thermo-mechanical fatigue life analysis.

3.5. Validation

The FEA results indicate that the bridge area between intake and exhaust valves is a critical area with the maximum Von-Mises stress and lowest thermo-mechanical fatigue life. Therefore, this region would be the most prone to initiating the crack in the cylinder head. Based on Figs. 10 and 14, the FEA analysis results are consistent with the experimental tests. Fig. 16 displays the cracked cylinder head in the empirical tests, in which the cracking sites can be observed in the area between the exhaust valves. The lower thickness and high temperature of the material due to the improper cooling led this area to tolerate the highest stress and eventually crack.

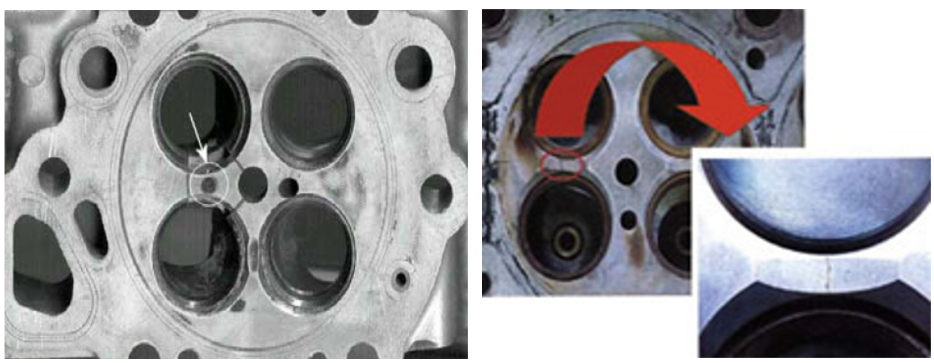

(a) (b)

Fig. 16. The cracked cylinder head, (a) [36], (b) [27]

The results of [32], which studied the thermo-mechanical analysis of the coated cylinder head, were employed to validate the thermo-mechanical analysis. This study predicted the highest temperature (308°C) at the bridge area between intake and exhaust valves, which is similar to the present study and shows a very good fit. In Fig. 17, the temperature variations at the bridge between intake and exhaust valves, which is considered a critical area due to the thermal analysis, are compared with the results of [32], suggesting a very good fit. The maximum stress of 134 MPa was predicted at the bridge between intake and exhaust valves in [20]. Notably, the maximum stress in the present study was 136 MPa at the same area. Such a 2 MPa (approximately 1.5%) discrepancy in the mechanical analysis results shows their appropriate fit.

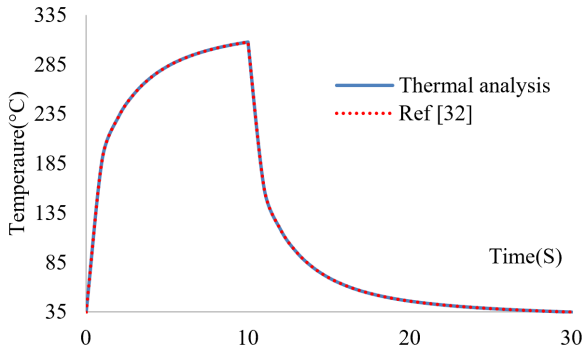

Fig. 17. Comparison of temperature changes at the critical node with the results of source [32]

4. Conclusions

The present study evaluated the impact of viscous behavior on the thermo-mechanical fatigue life of the engine cylinder head using the Sehitoglu model. The viscous behavior was considered using a two-layer viscoplasticity model. The viscous and mechanical properties and parameters of the Chabouche's isotropic-kinematic nonlinear hardening pattern for aluminum-silicon-magnesium alloy were calculated using LCF tests at various temperatures. LCF tests were simulated by ANSYS software, and an excellent agreement was shown between the experimental and simulation results of LCF tests. The finite element analysis revealed that the highest temperature and stress values were 308°C and 136 MPa, and the position is at the valve bridge. According to the thermo-mechanical analysis, the region between the intake and exhaust valves is a critical area and prone to fatigue cracks. The mechanical analysis suggested that excluding the viscous behavior leads to an underestimation of Von-Mises stress by 5.8 MPa (4.3%). The TMF life with and without considering the viscous behavior impact was calculated as 7407 and 8064 cycles, respectively. As FEM analysis results suggested, excluding the impact of viscous behavior leads to an overestimation of the thermomechanical fatigue life of the cylinder head by 657 cycles (≅ 8.9%), highlighting its significant effect. The simulation results were compared with the thermomechanical analysis of [32], showing a very good fit. The simulation results were also compared with a real damaged cylinder head to validate the FEA results, indicating the appropriate correspondence between the critical areas and rupture areas in the damaged sample.

References

[1] Y. Li, J. Liu, G. Zhong, W. Huang, and R. Zou. Analysis of a diesel engine cylinder head failure caused by casting porosity defects. *Engineering Failure Analysis*, 127:1–14, 2021. doi: 10.1016/j.engfailanal.2021.105498.

[2] G. Jing, Z. Ly, Y. Liu, S. Xiao, H. Zhou, and S. Li. Reliability study for diesel engine cylinder head through fatigue failure analysis and structural optimization. *Engineering Failure Analysis*, 142:1–14, 2022. doi: 10.1016/j.engfailanal.2022.106768.

[3] X. Luo, X. Zeng, P. Zou, Y. Lin, T. Wei, X. Yuan and S. Liao. A finite element analysis computational fluid dynamics coupled analysis on thermal-mechanical fatigue of cylinder head of a turbo-charged diesel engine. *Journal of Automobile Engineering*, 234(6):1–10, 2019. doi: 10.1177/0954407019890481.

[4] P.R. Ren, W. Song, G. Zhong, W.Q. Huang, Z.X. Zuo, C.Z. Zhao, and K.J. Yan. High-cycle fatigue failure analysis of cast Al-Si alloy engine cylinder head. *Engineering Failure Analysis*, 127:1–15, 2021. doi: 10.1016/j.engfailanal.2021.105546.

[5] R. Hazime, T. Seifert, and J. Kessens. Lifetime Assessment of Cylinder Heads for Efficient Heavy Duty Engines Part II: Component-Level Application of Advanced Models for Thermo-mechanical Fatigue Life Prediction of Lamellar Graphite Cast Iron GJL250 and Vermicular Graphite Cast Iron GJV450 Cylinder Heads. *SAE Technical Paper* No. 2017-01-0346, 2017. doi: 10.4271/2017-01-0346.

[6] Y. Liu, P. Annabattula, S. Mirmiran, L. Zhang, J. Chen, S. Gaikwad, and K. Singh. Assessing Thermo-mechanical Fatigue of a Cast Aluminum Alloy Cylinder Head of an Internal Combustion Engine, *SAE Technical Paper* No. 2020-01-1077, 2020. doi: 10.4271/2020-01-1077.

[7] H. Ashouri, B. Beheshti, and M. R. Ebrahimzadeh. Analysis of fatigue cracks of diesel engines cylinder heads. *Journal of Theoretical and Applied Mechanic*, 54(1):369–383, 2015. doi: 10.15632/jtam-pl.54.2.369.

[8] H. Ashouri. Thermal barrier coating effect on stress and temperature distribution of diesel engines cylinder heads using a two layer viscoelasticity model with considering viscosity. *International Journal of Automotive Engineering*, 7(2):2380–2392, 2017. doi: 10.22068/ijae.7.2.2380.

[9] W. Yang, J. Pang, L. Wang, X. Kang, S. Zhou, C. Zou, S. Li, and Z. Zhang. Thermo-mechanical fatigue life prediction based on the simulated component of cylinder head. *Engineering Failure Analysis*, 135:1–13, 2022. doi: 10.1016/j.engfailanal.2022.106105.

[10] A. Basiri and A, Amini. On the Service Life Prediction of Diesel Engine Cylinder Head under Thermomechanical Fatigue Loading with Several Damage Models: A Comparative Study. *Automotive Science and Engineering*, 12(1):3772–3786, 2022. doi: 10.22068/ase.2022.578.

[11] R. Hazime, C. C. Chang, Q. Wang, and S. Sochor. Thermomechanical Fatigue Life Predictions of Cast Aluminum Cylinder Heads Considering Defect Distribution. *SAE Technical Paper* No. 2023-01-0594, 2023. doi: 10.4271/2023-01-0594.

[12] G. Jing, S. Li, S. Xiao, T. Ma, Z. Ly, S. Sun, and H. Zhou. Research on fatigue reliability assessment of engine cylinder head based on neural network. *International Journal of Fatigue*, 175:1–19, 2023. doi: 10.1016/j.ijfatigue.2023.107800.

[13] H. Ashouri. Evaluation of quenching process on low cycle fatigue life for cylinder head. *Automotive Science Engineering*, 12(4):3971–3979, 2022. doi: 10.22068/ase.2022.613.

[14] H. Ashouri. Low cycle fatigue prediction for cylinder heads considering stress gradient and local yielding. *Proceedings of the Institution of Mechanical Engineers, Part D: Journal of Automobile Engineering*, 239(6):2153–2162, 2025. doi: 10.1177/09544070241228781.

[15] H. Zhang, Y. Cui, G. Liang, L. Li, G. Zhang, and X. Qiao. Fatigue life prediction analysis of high intensity marine diesel engine cylinder head based on fast thermal fluid solid coupling method. *Journal of the Brazilian Society of Mechanical Sciences and Engineering*, 43:1–15, 2021. doi: 10.1007/s40430-021-03049-7.

[16] P. Mahajan, A. Thakur, and R. Bodake. Correlation of Experimental Thermal Mapping and FEA Thermal Simulation for Cylinder Head for Diesel Engine Development. *SAE Technical Paper* No. 2020-28-0353, 2020. doi: 10.4271/2020-28-0353.

[17] T. Seifert T, R. Hazime, C.C. Chang, and C. Hu. Constitutive Modeling and Thermo-mechanical Fatigue Life Predictions of A356-T6 Aluminum Cylinder Heads Considering Ageing Effects. *SAE Technical Paper* No. 2019-01-0534, 2019. doi: 10.4271/2019-01-0534.

[18] X. Zeng, X. Luo, G. Jing, P. Zou, Y. Lin, T. Wei, X. Yuan , and H. Ge. Engine Cylinder Head Thermal-Mechanical Fatigue Evaluation Technology and Platform Application. *SAE International Journal of Engines*, 13(1):101–120, 2020. doi: 10.4271/03-13-01-0008.

[19] A. Pingale, C. C. Chang, and J. Perander. Data Driven Model to Predict Cylinder Head Fatigue Failure. *SAE Technical Paper* No. 2021-01-0801, 2021. doi: 10.4271/2021-01-0801.

[20] H. Blondet and K. Barthoux. Fatigue software improvement for calculating by FEA a complete map of the damage due to a duty cycle, regarding thermo-mechanical failure mode. *Procedia Structural Integrity*, 38:526–537, 2022. doi: 10.1016/j.prostr.2022.03.053.

[21] P. Mahajan, R. Bodake, and A. Thakur. Optimization of Scallop Design for Cylinder Head of a Multi-Cylinder Diesel Engine for Reduction of Combustion Deck Temperatures and Simultaneously Enhancing Combustion Deck Fatigue Margin. *SAE Technical Paper* 2021-01-1233, 2021. doi: 10.4271/2021-01-1233.

[22] M. Beranger, J.M. Fiark, K. Ammar, and G. Calletaud. A new fatigue model including thermal ageing for low copper aluminum-silicon alloys. *Procedia Engineering*, 213:720–729, 2018. doi: 10.1016/j.proeng.2018.02.068

[23] H. Ashouri. Evaluation of Fatigue, Oxidation and Creep Damages on Thermo-mechanical Fatigue Life for Cylinder Heads. *AUT Journal of Mechanical Engineering*, 9(3):281–294, 2025. doi: 10.22060/ajme.2025.23540.6142.

[24] H. Ashouri. Effect of viscosity stress on the low cycle fatigue of the cylinder head. *Amirkabir Journal of Mechanical Engineering*, 56(8):1053–1074, 2024. doi: 10.22060/mej.2024.23563.7782.

[25] F. Huang, W. CAI, Z. Zhang, W. Zhang, L. Shi, X. Li, B. Kaltenegger, D. Suzzi, W. Schrei, and K. Weihrauch. Cylinder Head Structure Optimization Simulation Study based on Sub-Model Method. *SAE Technical Paper* No. 2017-01-2433, 2017. doi: 10.4271/2017-01-2433.

[26] A. Piergiacomi, S.G. Barbieri, F. Renso, V. Mangeruga, and M. Giacopini. Investigation via Finite Element Analysis of the Influence of Boiling on the Thermo-Structural Behavior of the Engine Head of a High-Performance Combustion Engine. *SAE Technical Paper* No. 2023-24-0184, 2023. doi: 10.4271/2023-24-0184.

[27] M. Angeloni. *Fatigue life evaluation of A356 aluminum alloy used for engine cylinder head*. Ph.D. Thesis, University of Sau Palu, Brazil, 2011.

[28] G.H. Farrahi, M. Ghodrati, M. Azadi, and M. Rezvani Rad. Stress-strain time-dependent behavior of A356.0 aluminum alloy subject to cyclic thermal and mechanical lading. *Journal of Mech Time-Depend Mater*, 18:475–491, 2014. doi: 10.1007/s11043-014-9238-4.

[29] A. Deshpande, S.B. Leen, and T.H. Hyde. Experimental and numerical characterization of the cyclic thermo-mechanical behavior of a high temperature forming tool alloy. *ASME Journal of Manufacturing Science and Engineering*, 132:1–12, 2010. doi: 10.1115/1.4002534.

[30] J.L. Chaboche. A review of some plasticity and viscoplasticity constitutive theories. *International Journal of Plasticity*, 24:1642–1693, 2008. doi: 10.1016/j.ijplas.2008.03.009.

[31] ABAQUS/CAE(v2021), 2021, User's Manual.

[32] M. Houseni. *The effect of thermal barrier coating on temperature and stress distribution in diesel engine cylinder head*. MSc. Thesis, Shahre-Rey Branch, Islamic Azad University, Tehran, Iran, 2017.

[33] R.W. Neu, and H. Sehitoglu. Thermomechanical Fatigue, Oxidation and Creep: Part I. *Damage Mechanism. Metall. Trans. A*, 20:1755–1776. 1989. doi: 10.1007/BF02663207.

[34] R.W. Neu, and H. Sehitoglu. Thermomechanical Fatigue, Oxidation and Creep: Part II. *Life Prediction. Metall. Trans. A*, 20:1769–1783, 1989. doi: 10.1007/BF02663208.

[35] R. Stephens, A. Fatemi, and H. Fuchs H. *Metal fatigue in engineering*, 2nd edition, John Wiley, 2001.

[36] T. Takahashi and T. Sasaki. Low cycle fatigue of aluminum alloy cylinder heads in consideration of changing metrology microstructure. *Journal of Procedia Engineering*, 2:767–776, 2010. doi: 10.1016/j.proeng.2010.03.083.